The Nuclear Level Density and the Determination of Thermonuclear Rates for Astrophysics

Thomas Rauscher
Institut für Physik, Universität Basel, Basel, Switzerland

Friedrich-Karl Thielemann
Institut für Physik, Universität Basel, Basel, Switzerland

Karl-Ludwig Kratz
Institut für Kernchemie, Universität Mainz, Germany

Abstract

The prediction of cross sections for nuclei far off stability is crucial in the field of nuclear astrophysics. In recent calculations the nuclear level density – as an important ingredient to the statistical model (Hauser-Feshbach) – has shown the highest uncertainties. We present a global parametrization of nuclear level densities within the back-shifted Fermi-gas formalism. Employment of an energy-dependent level density parameter a, based on microscopic corrections from a recent FRDM mass formula, and a backshift δ, based on pairing and shell corrections, leads to a highly improved fit of level densities at the neutron-separation energy in the mass range $20 \leq A \leq 245$. The importance of using proper microscopic corrections from mass formulae is emphasized. The resulting level description is well suited for astrophysical applications.

The level density can also provide clues to the applicability of the statistical model which is only correct for a high density of excited states. Using the above description, one can derive a "map" for the applicability of the model to reactions of stable and unstable nuclei with neutral and charged particles.

26.30.+k – 21.10.Ma – 24.60.Dr – 95.30.Cq

I. INTRODUCTION

Explosive nuclear burning in astrophysical environments produces unstable nuclei, which again can be targets for subsequent reactions. In addition, it involves a very large number of stable nuclei, which are not fully explored by experiments. Thus, it is necessary to be able to predict reaction cross sections and thermonuclear rates with the aid of theoretical models. Explosive burning in supernovae involves in general intermediate mass and heavy nuclei. Due to a large nucleon number they have intrinsically a high density of excited states. A high level density in the compound nucleus at the appropriate excitation energy allows to make use of the statistical model approach for compound nuclear reactions (e.g. [1,2,3]), which averages over resonances. In this paper, we want to present new results obtained within this approach and outline in a clear way, where its application is valid.

It is often colloquially termed that the statistical model is only applicable for intermediate and heavy nuclei. However, the only necessary condition for its application is a large number of resonances at the appropriate bombarding energies, so that the cross section can be described by an average over resonances. This can in specific cases be valid for light nuclei and on the other hand not be valid for intermediate mass nuclei near magic numbers. Thus, another motivation of this investigation is to explore the nuclear chart for reactions with a sufficiently high level density, implying automatically that the nucleus can equilibrate in the classical compound nucleus picture.

As the capture of an alpha particle leads usually to larger Q-values than neutron or proton captures, the compound nucleus is created at a higher excitation energy. Therefore, it is often even possible to apply the Hauser-Feshbach formalism for light nuclei in the case of alpha-captures. Another advantage of alpha-captures is that the capture Q-values vary very little with the N/Z-ratio of a nucleus, for nuclei with $Z \leq 50$. For $Z > 50$, entering the regime of natural alpha-decay, very small alpha-capture Q-values can be encountered for proton-rich nuclei. Such nuclei on the other hand do not play a significant role in astrophysical environments, maybe with exception of the p-process. This means that in the case of alpha-captures the requirement of large level densities at the bombarding energy is equally well fulfilled at stability as for unstable nuclei. Opposite to the behavior for alpha-induced reactions, the reaction Q-values for proton or neutron captures vary strongly with the N/Z-ratio, leading eventually to vanishing Q-values at the proton or neutron drip line. For small Q-values the compound nucleus is created at low excitation energies and also for intermediate nuclei the level density can be quite small. Therefore, it is not advisable to apply the statistical model approach close to the proton or neutron drip lines for intermediate nuclei. For neutron captures close to the neutron drip line in r-process applications it might be still permissable for heavy and often deformed nuclei, which have a high level density already at very low excitation energies.

In astrophysical applications usually different aspects are emphasized than in pure nuclear physics investigations. Many of the latter in this long and well established field were focused on specific reactions, where all or most "ingredients", like optical potentials for particle and alpha transmission coefficients, level densities, resonance energies and widths of giant resonances to be implementated in predicting E1 and M1 gamma-transitions, were deduced from experiments. This of course, as long as the statistical model prerequisites are met, will produce highly accurate cross sections.

For the majority of nuclei in astrophysical applications such information is not available. The real challenge is thus not the well established statistical model, but rather to provide all these necessary ingredients in as reliable a way as possible, also for nuclei where none of such informations are available. In addition, these approaches should be on a similar level as e.g. mass models, where the investigation of hundreds or thousands of nuclei is possible with managable computational effort, which is not always the case for fully microscopic calculations.

The statistical model approach has been employed in calculations of thermonuclear reaction rates for astrophysical purposes by many researchers [4,5,6,7], who in the beginning only made use of ground state properties. Later, the importance of excited states of the target was pointed out [8]. The compilations [9,10,11] are presently the ones utilized in large scale applications in all subfields of nuclear astrophysics, when experimental information is unavailable. Existing global optical potentials, mass models to predict Q-values, deformations etc., but also the ingredients to describe giant resonance properties have been quite successful in the past (see e.g. the review by [12]). The major remaining uncertainty in all existing calculations stems from the prediction of nuclear level densities, which in earlier calculations gave uncertainties even beyond a factor of 10 at the neutron separation energy [13], about a factor of 8 [10], and a factor of 5 even in the most recent calculations (e.g. [11]; see Fig.3.16 in [12]). In nuclear reactions the transitions to lower lying states dominate due to the strong energy dependence. Because the deviations are usually not as high yet at low excitation energies, the typical cross section uncertainties amounted to a smaller factor of 2–3.

We want to show in this paper, after a short description of the model and the required nuclear input, the implementation of a novel treatment of level density descriptions [14,15], where the level density parameter is energy dependent and shell effects vanish at high excitation energies. This is still a phenomenological approach, making use of a back-shifted Fermi-gas model, rather than a combinatorial approach based on microscopic single-particle levels. But it is the first one leading to a reduction of the average cross section uncertainty to a factor of about 1.4, i.e. an average deviation of about 40% from experiments, when only employing global predictions for all input parameters and no specific experimental knowledge. The degree of precision of the present approach will give astrophysical nucleosynthesis calculations a much higher predictive power. In order to give a guide for its application, we also provide a map of the nuclear chart which indicates where the statistical model requirements are fulfilled and its predictions therefore safe to use.

II. THERMONUCLEAR RATES FROM STATISTICAL MODEL CALCULATIONS

A. The basic procedure

A high level density in the compound nucleus permits to use averaged transmission coefficients T, which do not reflect a resonance behavior, but rather describe absorption via an imaginary part in the (optical) nucleon-nucleus potential [2]. This leads to the well known expression

$$\sigma_i^{\mu\nu}(j,o;E_{ij}) = \frac{\pi\hbar^2/(2\mu_{ij}E_{ij})}{(2J_i^\mu+1)(2J_j+1)} \times \sum_{J,\pi}(2J+1)\frac{T_j^\mu(E,J,\pi,E_i^\mu,J_i^\mu,\pi_i^\mu)T_o^\nu(E,J,\pi,E_m^\nu,J_m^\nu,\pi_m^\nu)}{T_{tot}(E,J,\pi)} \quad (1)$$

for the reaction $i^\mu(j,o)m^\nu$ from the target state i^μ to the exited state m^ν of the final nucleus, with a center of mass energy E_{ij} and reduced mass μ_{ij}. J denotes the spin, E the corresponding excitation energy in the compound nucleus and π the parity of excited states. When these properties are used without subscripts they describe the compound nucleus, subscripts refer to states of the participating nuclei in the reaction $i^\mu(j,o)m^\nu$ and superscripts indicate the specific excited states. Experiments measure $\sum_\nu \sigma_i^{0\nu}(j,o;E_{ij})$, summed over all excited states of the final nucleus, with the target in the ground state. Target states μ in an astrophysical plasma are thermally populated and the astrophysical cross section $\sigma_i^*(j,o)$ is given by

$$\sigma_i^*(j,o;E_{ij}) = \frac{\sum_\mu(2J_i^\mu+1)\exp(-E_i^\mu/kT)\sum_\nu\sigma_i^{\mu\nu}(j,o;E_{ij})}{\sum_\mu(2J_i^\mu+1)\exp(-E_i^\mu/kT)} \quad . \quad (2)$$

The summation over ν replaces $T_o^\nu(E,J,\pi)$ in Eq. 1 by the total transmission coefficient

$$T_o(E,J,\pi) = \sum_{\nu=0}^{\nu_m} T_o^\nu(E,J,\pi,E_m^\nu,J_m^\nu,\pi_m^\nu) + \int_{E_m^{\nu_m}}^{E-S_{m,o}} \sum_{J_m,\pi_m} T_o(E,J,\pi,E_m,J_m,\pi_m)\rho(E_m,J_m,\pi_m)dE_m \quad . \quad (3)$$

Here $S_{m,o}$ is the channel separation energy, and the summation over excited states above the highest experimentally known state ν_m is changed to an integration over the level density ρ. The summation over target states μ in Eq. 2 has to be generalized accordingly.

In addition to the ingredients required for Eq. 1, like the transmission coefficients for particles and photons, width fluctuation corrections $W(j,o,J,\pi)$ have to be employed. They define the correlation factors with which all partial channels for an incoming particle j and outgoing particle o, passing through the excited state (E,J,π), have to be multiplied. This takes into account that the decay of the state is not fully statistical, but some memory of the way of formation is retained and influences the available decay choices. The major effect is elastic scattering, the incoming particle can be immediately re-emitted before the nucleus equilibrates. Once the particle is absorbed and not re-emitted in the very first (pre-compound) step, the equilibration is very likely. This corresponds to enhancing the elastic channel by a factor W_j. In order to conserve the total cross section, the individual transmission coefficients in the outgoing channels have to be renormalized to T_j'. The total cross section is proportional to T_j and, when summing over the elastic channel (W_jT_j') and all outgoing channels ($T_{tot}'-T_j'$), one obtains the condition $T_j{=}T_j'(W_jT_j'/T_{tot}')+T_j'(T_{tot}'-T_j')/T_{tot}'$. We can (almost) solve for T_j'

$$T_j' = \frac{T_j}{1+T_j'(W_j-1)/T_{tot}'} \quad . \quad (4)$$

This requires an iterative solution for T' (starting in the first iteration with T_j and T_{tot}), which converges fast. The enhancement factor W_j has to be known in order to apply Eq. 4. A general expression in closed form was derived [16], but is computationally expensive to use. A fit to results from Monte Carlo calculations gave [17]

$$W_j = 1 + \frac{2}{1 + T_j^{1/2}} \quad . \tag{5}$$

For a general discussion of approximation methods see [3,18]. Eqs. 4 and 5 redefine the transmission coefficients of Eq. 1 in such a manner that the total width is redistributed by enhancing the elastic channel and weak channels over the dominant one. Cross sections near threshold energies of new channel openings, where very different channel strengths exist, can only be described correctly, when taking width fluctuation corrections into account. Of the thermonuclear rates presently available in the literature, only those by Thielemann et al. [11] include this effect, but their level density treatment still contains large uncertainties. The width fluctuation corrections of [17] are only an approximation to the correct treatment. However, it was shown that they are quite adequate [19].

The important ingredients of statistical model calculations as indicated in Eqs. 1 through 3 are the particle and gamma-transmission coefficients T and the level density of excited states ρ. Therefore, the reliability of such calculations is determined by the accuracy with which these components can be evaluated (often for unstable nuclei). In the following we want to discuss the methods utilized to estimate these quantities and recent improvements.

B. Transmission Coefficients

The transition from an excited state in the compound nucleus (E, J, π) to the state $(E_i^\mu, J_i^\mu, \pi_i^\mu)$ in nucleus i via the emission of a particle j is given by a summation over all quantum mechanically allowed partial waves

$$T_j^\mu(E, J, \pi, E_i^\mu, J_i^\mu, \pi_i^\mu) = \sum_{l=|J-s|}^{J+s} \sum_{s=|J_i^\mu - J_j|}^{J_i^\mu + J_j} T_{j_{ls}}(E_{ij}^\mu). \tag{6}$$

Here the angular momentum $\vec{l}$ and the channel spin $\vec{s} = \vec{J}_j + \vec{J}_i^\mu$ couple to $\vec{J} = \vec{l} + \vec{s}$. The transition energy in channel j is $E_{ij}^\mu = E - S_j - E_i^\mu$.

The individual particle transmission coefficients T_l are calculated by solving the Schrödinger equation with an optical potential for the particle-nucleus interaction. All early studies of thermonuclear reaction rates [4,6,8,7,9,10] employed optical square well potentials and made use of the black nucleus approximation. We employ the optical potential for neutrons and protons given by [20], based on microscopic infinite nuclear matter calculations for a given density, applied with a local density approximation. It includes corrections of the imaginary part [21,22]. The resulting s-wave neutron strength function $< \Gamma^o/D > |_{1\mathrm{eV}} = (1/2\pi) T_{n(l=0)}(1\mathrm{eV})$ is shown and discussed in [23,12], where several phenomenological optical potentials of the Woods-Saxon type and the equivalent square well potential used in earlier astrophysical applications are compared. The purely theoretical approach gives the best fit. It is also expected to have the most reliable extrapolation properties for unstable nuclei. A good overview on different approaches can be found in [24].

Deformed nuclei were treated in a very simplified way by using an effective spherical potential of equal volume, based on averaging the deformed potential over all possible angles between the incoming particle and the orientation of the deformed nucleus.

In most earlier compilations alpha particles were also treated by square well optical potentials. We employ a phenomenological Woods-Saxon potential [25] based on extensive data [26]. For future use, for alpha particles and heavier projectiles, it is clear that the best results can probably be obtained with folding potentials (e.g. [27,28,29]).

The gamma-transmission coefficients are treated as follows. The dominant gamma-transitions (E1 and M1) have to be included in the calculation of the total photon width. The smaller, and therefore less important, M1 transitions have usually been treated with the simple single particle approach ($T \propto E^3$ [30]), as also discussed in [9]. The E1 transitions are usually calculated on the basis of the Lorentzian representation of the Giant Dipole Resonance (GDR). Within this model, the E1 transmission coefficient for the transition emitting a photon of energy E_γ in a nucleus ${}^A_N Z$ is given by

$$T_{E1}(E_\gamma) = \frac{8}{3}\frac{NZ}{A}\frac{e^2}{\hbar c}\frac{1+\chi}{mc^2}\sum_{i=1}^{2}\frac{i}{3}\frac{\Gamma_{G,i}E_\gamma^4}{(E_\gamma^2 - E_{G,i}^2)^2 + \Gamma_{G,i}^2 E_\gamma^2} \quad . \tag{6}$$

Here $\chi(= 0.2)$ accounts for the neutron-proton exchange contribution [31] and the summation over i includes two terms which correspond to the split of the GDR in statically deformed nuclei, with oscillations along (i=1) and perpendicular (i=2) to the axis of rotational symmetry. Many microscopic and macroscopic models have been devoted to the calculation of the GDR energies (E_G) and widths (Γ_G). Analytical fits as a function of A and Z were also used [9,10]. We make use of the (hydrodynamic) droplet model approach [32] for E_G, which gives an excellent fit to the GDR energies and can also predict the split of the resonance for deformed nuclei, when making use of the deformation, calculated within the droplet model. In that case, the two resonance energies are related to the mean value calculated by the relations [33] $E_{G,1} + 2E_{G,2} = 3E_G$, $E_{G,2}/E_{G,1} = 0.911\eta + 0.089$. η is the ratio of the diameter along the nuclear symmetry axis to the diameter perpendicular to it, and can be obtained from the experimentally known deformation or mass model predictions.

See [12] for a detailed description of the approach utilized to calculate the gamma-transmission coefficients for the cross section determination shown in this work.

III. LEVEL DENSITIES

A. The Back-Shifted Fermi-Gas Model

While the method as such is well seasoned, considerable effort has been put into the improvement of the input for statistical Hauser-Feshbach models (e.g. [12]). However, the nuclear level density has given rise to the largest uncertainties in the description of nuclear reactions [12,9,11,34]. For large scale astrophysical applications it is also necessary to not only find reliable methods for level density predictions, but also computationally feasible ones.

Such a model is the non-interacting Fermi-gas model [35]. Most statistical model calculations use the back-shifted Fermi-gas description [13]. More sophisticated Monte Carlo

shell model calculations [36], as well as combinatorial approaches (see e.g. [37]), have shown excellent agreement with this phenomenological approach and justified the application of the Fermi-gas description at and above the neutron separation energy. Here we want to apply an energy-dependent level density parameter a together with microscopic corrections from nuclear mass models, which leads to improved fits in the mass range $20 \leq A \leq 245$.

Mostly the back-shifted Fermi-gas description, assuming an even distribution of odd and even parities (however, see e.g. [38] for doubts on the validity of this assumption at energies of astrophysical interest), is used [13]:

$$\rho(U,J,\pi) = \frac{1}{2}\mathcal{F}(U,J)\rho(U) \quad , \tag{7}$$

with

$$\rho(U) = \frac{1}{\sqrt{2\pi}\sigma}\frac{\sqrt{\pi}}{12a^{1/4}}\frac{\exp(2\sqrt{aU})}{U^{5/4}} \ , \qquad \mathcal{F}(U,J) = \frac{2J+1}{2\sigma^2}\exp\left(\frac{-J(J+1)}{2\sigma^2}\right) \tag{8}$$

$$\sigma^2 = \frac{\Theta_{\rm rigid}}{\hbar^2}\sqrt{\frac{U}{a}} \ , \qquad \Theta_{\rm rigid} = \frac{2}{5}m_{\rm u}AR^2 \ , \qquad U = E - \delta \quad .$$

The spin dependence $\mathcal{F}$ is determined by the spin cut-off parameter σ. Thus, the level density is dependent on only two parameters: the level density parameter a and the backshift δ, which determines the energy of the first excited state.

Within this framework, the quality of level density predictions depends on the reliability of systematic estimates of a and δ. The first compilation for a large number of nuclei was provided by [13]. They found that the backshift δ is well reproduced by experimental pairing corrections. They also were the first to identify an empirical correlation with experimental shell corrections $S(N,Z)$

$$\frac{a}{A} = c_0 + c_1 S(N,Z) \quad , \tag{9}$$

where $S(N,Z)$ is negative near closed shells. Since then, a number of compilations have been published and also slightly different functional dependencies have been proposed (for references, see e.g. [12]), but they did not necessarily lead to better predictive power.

Improved agreement with experimental data was found [11,34] by dividing the nuclei into three classes [(i) those within three units of magic nucleon numbers, (ii) other spherical nuclei, (iii) deformed nuclei] and fitting separate coefficients c_0, c_1 for each class. In that case the mass formula in Ref. [39] was used. For the backshift δ the description

$$\delta = \Delta(Z,N) \tag{10}$$

was employed, deriving $\Delta(Z,N)$ from the pairing correlation of a droplet model nuclear mass formula with the values

$$\begin{aligned} \Delta_{\rm even-even} &= \frac{12}{\sqrt{A}} \quad , \\ \Delta_{\rm odd} &= 0 \quad , \\ \Delta_{\rm odd-odd} &= -\frac{12}{\sqrt{A}} \quad . \end{aligned} \tag{11}$$

With this treatment smaller deviations were found, compared to previous attempts [13,9]. However, the number of parameters was considerably increased at the same time.

The back-shifted Fermi-gas approach diverges for $U = 0$ (i.e. $E = \delta$, if δ is a positive backshift). In order to get the correct behavior at very low excitation energies, the Fermi-gas description can be combined with the constant temperature formula ([13]; [3] and references therein)

$$\rho(U) \propto \frac{\exp(U/T)}{T} \quad . \tag{12}$$

The two formulations are matched by a tangential fit determining T.

B. Thermal Damping of Shell Effects

An improved approach has to consider the energy dependence of the shell effects which are known to vanish at high excitation energies [14]. Although, for astrophysical purposes only energies close to the particle separation thresholds have to be considered, an energy dependence can lead to a considerable improvement of the global fit. This is especially true for strongly bound nuclei close to magic numbers.

An excitation-energy dependent description was initially proposed by [40,15] for the level density parameter a:

$$a(U, Z, N) = \tilde{a}(A) \left[1 + C(Z, N) \frac{f(U)}{U} \right] \quad , \tag{13}$$

where

$$\tilde{a}(A) = \alpha A + \beta A^{2/3} \tag{14}$$

and

$$f(U) = 1 - \exp(-\gamma U) \quad . \tag{15}$$

The values of the free parameters α, β and γ are determined by fitting to experimental level density data.

The shape of the function $f(U)$ permits the two extremes: (i) for small excitation energies the original form of Eq. 9 is retained with $S(Z, N)$ being replaced by $C(Z, N)$, (ii) for high excitation energies a/A approaches the continuum value obtained for infinite nuclear matter. Previous attempts to find a global description of level densities used shell corrections S derived from comparison of liquid-drop masses with experiment ($S \equiv M_{\rm exp} - M_{\rm LD}$) or the "empirical" shell corrections $S(Z, N)$ given by [13]. A problem connected with the use of liquid-drop masses arises from the fact that there are different liquid-drop model parametrizations available in the literature which produce quite different values for S [43].

However, in addition the meaning of the correction parameter inserted into the level density formula (Eq. 13) has to be reconsidered. The fact that nuclei approach a spherical shape at high excitation energies has to be included. Actually, the correction parameter C should describe properties of a nucleus differing from the *spherical* macroscopic energy and

include terms which are vanishing at higher excitation energies. The latter requirement is mimicked by the form of Eq. 13. Therefore, the parameter should rather be identified with the so-called "microscopic" correction $E_{\rm mic}$ than with the shell correction. The mass of a nucleus with deformation ϵ can then be written as [44]

$$M(\epsilon) = E_{\rm mic}(\epsilon) + E_{\rm mac}({\rm spherical}) \quad . \tag{16}$$

Alternatively, one can write

$$M(\epsilon) = E_{\rm mac}(\epsilon) + E_{\rm s+p}(\epsilon) \quad , \tag{17}$$

with $E_{\rm s+p}$ being the shell-plus-pairing correction. The confusion about the term "microscopic correction", which is sometimes used in an ambiguous way, is also pointed out in [44]. Thus, the above mentioned ambiguity follows from the inclusion of deformation-dependent effects into the macroscopic part of the mass formula.

Another important ingredient is the pairing gap Δ, related to the backshift δ. Instead of assuming constant pairing (cf. [41]) or a fixed dependence on the mass number A (cf. Eq. 11), we determine the pairing gap Δ from differences in the binding energies (or mass differences, respectively) of neighboring nuclei. Thus, for the neutron pairing gap $\Delta_{\rm n}$ one obtains [42]

$$\Delta_{\rm n}(Z,N) = \frac{1}{2}\left[2E^G(Z,N) - E^G(Z,N-1) - E^G(Z,N+1)\right] \quad , \tag{18}$$

where $E^G(Z,N)$ is the binding energy of the nucleus (Z,N). Similarly, the proton pairing gap $\Delta_{\rm p}$ can be calculated.

At low energies, this description is again combined with the constant temperature formula (Eq. 12) as described above.

C. Results

In our study we utilized the microscopic correction of a most recent mass formula [44], calculated with the Finite Range Droplet Model FRDM (using a folded Yukawa shell model with Lipkin-Nogami pairing) in order to determine the parameter $C(Z,N)$=$E_{\rm mic}$. The backshift δ was calculated by setting $\delta(Z,N)$=$1/2\{\Delta_{\rm n}(Z,N) + \Delta_{\rm p}(Z,N)\}$ and using Eq. 18. In order to obtain the parameters α, β, and γ, we performed a fit to experimental data on s-wave neutron resonance spacings of 272 nuclei at the neutron separation energy. The data were taken from a recent compilation [14]. Another recent investigation [43] also attempted to fit level density parameters, but made use of a slightly different description of the energy dependence of a and different pairing gaps.

As a quantitative overall estimate of the agreement between calculation and experiment, one usually quotes the averaged ratio [13,14]

$$g \equiv \left\langle \frac{\rho_{\rm calc}}{\rho_{\rm exp}} \right\rangle = \exp\left[\frac{1}{n}\sum_{i=1}^{n}\left(\ln\frac{\rho^i_{\rm calc}}{\rho^i_{\rm exp}}\right)^2\right]^{1/2} \quad , \tag{19}$$

with n being the number of nuclei for which level densities ρ are experimentally known.

As best fit we obtain an averaged ratio $g = 1.48$ with the parameter values $\alpha = 0.1337$, $\beta = -0.06571$, $\gamma = 0.04884$. The ratios of experimental to predicted level densities (i.e. theoretical to experimental level spacings) for the nuclei considered are shown in Fig. 1. As can be seen, for the majority of nuclei the absolute deviation is less than a factor of 2. This is a satisfactory improvement over the theoretical level densities previously used in astrophysical cross section calculations, where deviations of a factor 3–4 [11,34], or even in excess of a factor of 10 [12,9] were found. Such a direct comparison was rarely shown in earlier work. Mostly the level density parameter a, entering exponentially into the level density, was displayed. Closely examining the nuclei with the largest deviations in our fit, we were not able to find any remaining correlation of the deviation with separation energy (i.e. excitation energy) or spin.

Although we quoted the value of the parameter β above (and will do so below) as we left it as an open parameter in our fits, one can see that it is always small and can be set to zero without considerable increase in the obtained deviation. Therefore, it is obvious that actually only two parameters are needed for the level density description.

As an alternative to the FRDM mass formula [44], in Fig. 2 we show the results when making use of the well-known mass formula by Hilf et al. [39] which turned out to be successful in predicting properties of nuclei at and close to stability. The parameter set $\alpha = 0.0987$, $\beta = 0.09659$, $\gamma = 0.05368$ yields an averaged ratio of $g = 2.08$. It can be seen from Fig. 2 that not only the average scatter is somewhat larger than with the FRDM input, but also that this mass formula has problems in the higher mass regions. Only an artificial alteration by about -3 MeV or more of the microscopic term in the deformed mass regions $80 \leq N \leq 86$ and $103 \leq N \leq 113$ can slightly improve the fit but the remaining scatter still leads to $g = 1.85$. The difference in the calculated level density from the FRDM and the Hilf mass formulae is plotted in Fig. 3. The latter mass formula leads to a significantly higher level density (by about a factor of 10) around the neutron magic number $N = 82$, whereas the level density remains lower (by a factor of 0.07) close to the drip lines for $N > 115$.

A fit comparable to the quality of the FRDM approach can be obtained when employing a mass formula from an extended Thomas-Fermi plus Strutinsky integral model (ETFSI) [45]. In order to extract a microscopic correction for this already microscopic calculation, we subtracted the FRDM spherical macroscopic part $E_{\rm mac}$ (see Eq. 16) from the ETFSI mass and took this difference to be the ETFSI microscopic correction. The pairing gaps were calculated as described above. This leads to a fit with $g = 1.61$, yielding the parameter values $\alpha = 0.12682$, $\beta = -0.03652$ and $\gamma = 0.045$. However, although the fit is closer to the one obtained with FRDM than the Hilf result, the deviations for unstable nuclei are somewhat larger. The maximum deviation is a factor of about 38 for ETFSI, as compared to a factor of 16 for the Hilf approach. Both formulae yield lower level densities than the FRDM for nuclei close to the dripline with $N > 130$ and higher level densities for neutron rich nuclei close to the magic shell at $N = 82$. The ratios of the level density from the ETFSI approach to those of the FRDM are shown in Fig. 4.

Different combinations of masses and microscopic corrections from other models (droplet model by Myers and Swiatecki [46], Cameron-Elkin mass formula and shell corrections [47]) were also tried but did not lead to better results. Our fit to experimental level densities is also better than a recent analytical BCS approach [48,49] which tried to implement level spacings from the ETFSI model in a consistent fashion.

To see the effect of the new level density description (utilizing FRDM input) on the calculated cross sections, 30 keV neutron capture cross sections from experiment [50] are compared to our calculations in Fig. 5. Plotted are only nuclei for which the statistical model can be applied to calculate the cross section, using the criteria derived in the next section. An improvement in the overall deviation can be seen, compared to previous calculations [12]. However, one systematic deviation can clearly be seen in the $A \simeq 90$ region. That "peak" is not caused by a deficiency in the general level density description but by the microscopic input. The FRDM model overestimates the microscopic corrections close to the $N = 50$ shell [44].

We see that the uncertainty in level density translates into a similar uncertainty of the neutron capture cross sections which are used here as a representative example for applications to capture cross sections. Although this does not seem to be a dramatic improvement for the experimental cross sections of stable nuclei over the previous approach [11,34], the purely empirical and also artificial division of nuclei into three classes of level density treatments could be avoided. The reason is that the excitation energy dependence was treated in the generalized ansatz of [15], ensuring the correct energy dependence which will also yield correct results when the adjustment is not done at the typical separation energy of 8–12 MeV for stable nuclei but also for nuclei far from stability with smaller separation energies.

The remaining uncertainty in the extrapolation is the reliability far off stability of the nuclear-structure model from which the microscopic corrections and pairing gaps (and the masses) are taken. However, recent investigations in astrophysics and nuclear physics have shown the robustness of the FRDM approach [51]. Recently improved purely microscopic models have exhibited similar behavior towards the drip lines [52] but there are no large scale calculations over the whole chart of nuclei available yet which include deformation. Therefore, the FRDM model used here is among the most reliable ones available at present.

IV. APPLICABILITY OF THE STATISTICAL MODEL

Having a reliable level density description also permits to analyze when and where the statistical model approach is valid. Generally speaking, in order to apply the model correctly a sufficiently large number of levels in the compound nucleus is needed in the relevant energy range which can act as doorway states to forming a compound nucleus. In the following this is discussed for neutron-, proton- and alpha-induced reactions with the aid of the level density approach presented above. This section is intended to be a guide to a meaningful and correct application of the statistical model.

The nuclear reaction rate per particle pair at a given stellar temperature T is determined by folding the reaction cross section with the Maxwell-Boltzmann (MB) velocity distribution of the projectiles [54]

$$\langle \sigma v \rangle = \left(\frac{8}{\pi \mu} \right)^{1/2} \frac{1}{(kT)^{3/2}} \int_0^\infty \sigma(E) E \exp\left(-\frac{E}{kT} \right) dE \quad . \tag{20}$$

Two cases have to be considered: Reactions between charged particles and with neutrons.

A. The Effective Energy Window

The nuclear cross section for charged particles is strongely suppressed at low energies due to the Coulomb barrier. For particles having energies less than the height of the Coulomb barrier, the product of the penetration factor and the MB distribution function at a given temperature results in the so-called Gamow peak, in which most of the reactions will take place [53]. Location and width of the Gamow peak depend on the charges of projectile and target, and on the temperature of the interacting plasma.

When introducing the astrophysical S factor $S(E) = \sigma(E)E\exp(2\pi\eta)$ (with η being the Sommerfeld parameter), one can easily see the two contributions of the velocity distribution and the penetrability in the integral:

$$< \sigma v >= \left(\frac{8}{\pi\mu}\right)^{1/2} \frac{1}{(kT)^{3/2}} \int_0^\infty S(E) \exp\left[-\frac{E}{kT} - \frac{b}{E^{1/2}}\right] \quad , \tag{21}$$

where the quantity $b = (2\mu)^{1/2}\pi e^2 Z_1 Z_2/\hbar$ arises from the barrier penetrability. Taking the first derivative of the integrand yields the location of the Gamov peak E_0 [53,54],

$$E_0 = \left(\frac{bkT}{2}\right)^{2/3} = 1.22(Z_1^2 Z_2^2 \mu T_6^2)^{1/3}\,\mathrm{keV} \quad , \tag{22}$$

with the charges Z_1, Z_2 and the reduced mass μ of the involved nuclei at a temperature T_6 given in 10^6 K. The effective width Δ of the energy window can be derived as

$$\Delta = \frac{16E_0kT}{3}^{1/2} = 0.749(Z_1^2 Z_2^2 \mu T_6^5)^{1/6}\,\mathrm{keV} \quad . \tag{23}$$

In the case of neutron-induced reactions the effective energy window has to be derived in a slightly different way. For s-wave neutrons ($l = 0$) the energy window is simply given by the location and width of the peak of the MB distribution function. For higher partial waves the penetrability of the centrifugal barrier shifts the effective energy E_0 to higher energies, similar to the Gamov peak. For neutrons with energies less than the height of the centrifugal barrier this can be approximated by [56]

$$E_0 \approx 0.172T_9\left(l + \frac{1}{2}\right) \quad \mathrm{MeV}, \tag{24}$$

$$\Delta \approx 0.194T_9\left(l + \frac{1}{2}\right)^{1/2} \quad \mathrm{MeV}. \tag{25}$$

The energy E_0 will always be comparatively close to the neutron separation energy.

B. The Criterion for the Application of the Statistical Model

Using the above effective energy windows for charged and neutral particle reactions, a criterion for the applicability can be derived from the level density. For a reliable application of the statistical model a sufficient number of nuclear levels has to be within the energy window, thus contributing to the reaction rate. For narrow, isolated resonances, the cross

sections (and also the reaction rates) can be represented by a sum over individual Breit-Wigner terms. At higher energies, with increasing level density, the sum over resonances may be approximated by an integral over E [56].

Numerical test calculations were made in order to find the average number of levels per energy window which is sufficient to allow the substitution of the sum by an integral over the HF cross section. Fig. 6 shows the dependence of the ratio between sum and integral [56] on the number of levels in the energy window. To achieve 20% accuracy, about 10 levels are needed in the worst case (non-overlapping, narrow resonances). Usually, neutron s-wave resonances are comparatively broad and thus a smaller number of levels could be sufficient. However, applying the statistical model (i.e. integrating over a level density instead of summing up over levels) for a level density which is not sufficiently large, results in an overestimation of the actual cross section, as can be seen in Fig. 6 and was also shown in Ref. [55]. Therefore, in the following we will assume a conservative limit of 10 contributing resonances in the effective energy window for charged and neutral particle-induced reactions.

Fixing the required number of levels within the energy window of width Δ, one can find the minimum temperature at which the above described condition is fulfilled. Those temperatures (above which the statistical model can be used) are plotted in a logarithmic color scale in Figs. 7–8. For neutron-induced reactions Fig. 7 applies, Fig. 9 describes proton-induced reactions, and Fig. 8 alpha-induced reactions. Plotted is always the minimum stellar temperature T_9 (in 10^9 K) for the compound nucleus of the reaction. It should be noted that the derived temperatures will not change considerably even when changing the required level number within a factor of about two, because of the exponential dependence of the level density on the excitation energy.

This permits to read directly from the plot whether the statistical model cross section can be "trusted" or whether single resonances or other processes (e.g. direct reactions) have also to be considered. (However, this does not necessarily mean that the statistical cross section is always negligible in the latter cases, since the assumed condition is quite conservative). The above plots can give hints on when it is safe to use the statistical model approach and which nuclei have to be treated with special attention for specific temperatures. Thus, information on which nuclei might be of special interest for an experimental investigation may also be extracted.

V. SUMMARY

In the first part of the paper we described the most recent approaches being used for the application of statistical model calculations in astrophysical applications. In the second part we focussed on the level density description which contained the largest error when using the properties described before. We were able to improve considerably the prediction of nuclear level densities by employing an energy-dependent description for the level density parameter a and by properly including microscopic corrections and back-shifts. All nuclei can now be described with a single parameter set consisting of just three parameters. The globally averaged deviation of prediction from experiment of about 1.5 translates into a somewhat lower error in the final cross sections due to the dominance of transitions to states with low excitation energies. This will also make it worthwile to recalculate the cross sections and

thermonuclear rates for many astrophysically important reactions in the intermediate and heavy mass region.

Finally, we also presented a "map" as a guide for the application of the statistical model for neutron-, proton- and alpha-induced reactions. Figs. 7, 9, 8 (as well as Figs. 3, 4) as full size color plots can be obtained from the first author. The above plots can give hints on when it is safe to use the statistical model approach and which nuclei have to be treated with special attention at a given temperature. Thus, information on which nuclei might be of special interest for an experimental investigation may also be extracted. It should be noted that we used very conservative assumptions in deriving the above criteria for the applicability of the statistical model.

ACKNOWLEDGMENTS

We thank F. Käppeler and co-workers for making a preliminary version of their updated neutron-capture cross section compilation available to us. We also thank P. Möller for discussions. This work was supported in part by the Swiss Nationalfonds. TR is acknowledging support by the Austrian Academy of Sciences.

REFERENCES

[1] W. Hauser and H. Feshbach, *Phys. Rev. A* **87**, 366 (1952).
[2] C. Mahaux and H.A. Weidenmüller, *Ann. Rev. Part. Nucl. Sci.* **29**, 1 (1979).
[3] E. Gadioli and P.E. Hodgson, *Pre-Equilibrium Nuclear Reactions* (Clarendon Press, Oxford 1992).
[4] J.W. Truran, A.G.W. Cameron, and A. Gilbert, *Can. J. Phys.* **44**, 563 (1966).
[5] G. Michaud and W.A. Fowler, *Phys. Rev. C* **2**, 2041 (1970).
[6] G. Michaud and W.A. Fowler, *Ap. J.* **173**, 157 (1972).
[7] J.W. Truran, *Astrophys. Space Sci.* **18**, 308 (1972).
[8] M. Arnould, *Astron. Astrophys.* **19**, 92 (1972).
[9] J.A. Holmes, S.E. Woosley, W.A. Fowler, and B.A. Zimmerman, *At. Data Nucl. Data Tables* **18**, 306 (1976).
[10] S.E. Woosley, W.A. Fowler, J.A. Holmes, and B.A. Zimmerman, *At. Data Nucl. Data Tables* **22**, 371 (1978).
[11] F.-K. Thielemann, M. Arnould, and J.W. Truran, in *Advances in Nuclear Astrophysics*, eds. E. Vangioni-Flam et al., (Èditions Frontières, Gif-sur-Yvette 1987), p. 525.
[12] J.J. Cowan, F.-K. Thielemann, and J.W. Truran, *Phys. Rep.* **208**, 267 (1991).
[13] A. Gilbert and A.G.W. Cameron, *Can. J. Phys.* **43**, 1446 (1965).
[14] A.S. Iljinov, M.V. Mebel, N. Bianchi, E. De Sanctis, C. Guaraldo, V. Lucherini, V. Muccifora, E. Polli, A.R. Reolon, and P. Rossi, *Nucl. Phys.* **A543**, 517 (1992).
[15] A.V. Ignatyuk, K.K. Istekov, and G.N. Smirenkin, *Sov. J. Nucl. Phys.* **29**, 450 (1979).
[16] J.J.M. Verbaatschot, H.A. Weidenmüller, and M.R. Zirnbauer, *Phys. Rep.* **129**, 367 (1984).
[17] J.W. Tepel, H.M. Hoffmann, and H.A. Weidenmüller, *Phys. Lett.* **B49**, 1 (1974).
[18] S.N. Ezhov and V.A. Plujko, *Z. Phys.* **346**, 275 (1993).
[19] J. Thomas, M.R. Zirnbauer, and K.-H. Langanke, *Phys. Rev. C* **33**, 2197 (1986).
[20] J.P. Jeukenne, A. Lejeune, and C. Mahaux, *Phys. Rev. C* **16**, 80 (1977).
[21] S. Fantoni, B.L. Friman, and V.R. Pandharipande, *Phys. Rev. Lett.* **48**, 1089 (1981).
[22] C. Mahaux, *Phys. Rev. C* **82**, 1848 (1982).
[23] F.-K. Thielemann, J. Metzinger, and H.V. Klapdor, *Z. Phys. A* **309**, 301 (1983).
[24] R.L. Varner, W.J. Thompson, T.L. McAbee, E.J. Ludwig, and T.B. Clegg, *Phys. Rep.* **201**, 57 (1991).
[25] F.M. Mann, Hanford Engineering (**HEDL-TME 78-83**).
[26] L. McFadden and G.R. Satchler, *Nucl. Phys.* **84**, 177 (1966).
[27] A.K. Chaudhuri, D.N. Basu, and B. Sinha, *Nucl. Phys.* **A439**, 415 (1985).
[28] G.R. Satchler and W.G. Love, *Phys. Rep.* **55**, 183 (1979).
[29] H. Oberhummer, H. Herndl, T. Rauscher, and H. Beer, *Surveys in Geophys.* **17**, 665 (1996).
[30] J.M. Blatt and V.F. Weisskopf, *Theoretical Nuclear Physics* (Wiley, New York 1952).
[31] E. Lipparini and S. Stringari, *Phys. Rep.* **175**, 103 (1989).
[32] W.D. Myers, W.J. Swiatecki, T. Kodama, L.J. El-Jaick, and E.R. Hilf, *Phys. Rev. C* **15**, 2032 (1977).
[33] M. Danos, *Nucl. Phys.* **5**, 23 (1958).
[34] F.-K. Thielemann, M. Arnould, and J.W. Truran, in *Capture Gamma-Ray Spectroscopy*, eds. K. Abrahams, P. van Assche (IOP, Bristol 1988), p. 730.

[35] A.H. Bethe, *Phys. Rev.* **50**, 332 (1936).
[36] D.J. Dean, S.E. Koonin, K.-H. Langanke, P.B. Radha, and Y. Alhassid, *Phys. Rev. Lett.* **74**, 2909 (1995).
[37] V. Paar et al., *Proc. Int. Conf. Gamma-Ray Spectroscopy and Related Topics*, ed. G. Molnar (Springer Hungarica), in press.
[38] B. Pichon, *Nucl. Phys.* **A568**, 553 (1994).
[39] E.R. Hilf, H. von Groote, and K. Takahashi, in *Proc. Third Int. Conf. on Nuclei far from Stability*, (CERN **76**-13, Geneva), p. 142.
[40] A.V. Ignatyuk, G.N. Smirenkin, and A.S. Tishin, *Yad. Phys.* **21**, 485 (1975).
[41] Reisdorf, *Z. Phys. A* **300**, 227 (1981).
[42] R.-P. Wang, F.-K. Thielemann, D.H. Feng, and C.-L. Wu, *Phys. Lett. B* **284**, 196 (1992).
[43] A. Mengoni and Y. Nakajima, *J. Nucl. Sci. Techn.* **31**, 151 (1994).
[44] P. Möller, J.R. Nix, W.D. Myers, and W.J. Swiatecki, *At. Data Nucl. Data Tables* **59**, 185 (1995).
[45] Y. Aboussir, J.M. Pearson, A.K. Dutta, and F. Tondeur, *At. Data Nucl. Data Tables* **61**, 127 (1995).
[46] W.D. Myers and W.J. Swiatecki, *Ann. Phys.* **55**, 395 (1969).
[47] A.G.W. Cameron and R.M. Elkin, *Can. J. Phys.* **43**, 1288 (1965).
[48] S. Goriely, *Nucl. Phys.* **A605**, 28 (1996).
[49] S. Goriely, *Proc. Int. Conf. Gamma-Ray Spectroscopy and Related Topics*, ed. G. Molnar (Springer Hungarica), in press.
[50] Z.Y. Bao and F. Käppeler, private communication.
[51] F.-K. Thielemann, K.-L. Kratz, B. Pfeiffer, T. Rauscher, L. van Wormer, and M. Wiescher, *Nucl. Phys.* **A570**, 329c (1994).
[52] J. Dobaczewski, I. Hamamoto, W. Nazarewicz, and J.A. Sheikh, *Phys. Rev. Lett.* **72**, 981 (1994).
[53] C.E. Rolfs and W.S. Rodney, *Cauldrons in the Cosmos* (University of Chicago Press, Chicago 1988).
[54] W.A. Fowler, G.E. Caughlan, and B.A. Zimmerman, *Ann. Rev. Astron. Astrophys.* **5**, 525 (1967).
[55] L. van Wormer, J. Görres, C. Iliades, M. Wiescher, and F.-K. Thielemann, *Ap. J.* **432**, 326 (1994).
[56] R.V. Wagoner, *Ap. J. Suppl.* **18**, 247 (1969).

FIGURES

FIG. 1. Ratio of predicted to experimental [14] level densities at the neutron separation energy. The deviation is less than a factor of 2 (dotted lines) for the majority of the considered nuclei.

FIG. 2. Ratio of predicted to experimental [14] level densities at the neutron separation energy when using microscopic corrections from the Hilf mass formula [39].

FIG. 3. Ratio of the level density at the neutron separation energy calculated with microscopic corrections from Hilf et al [39] to those calculated using corrections from FRDM [44].

FIG. 4. Ratio of the level density at the neutron separation energy calculated with microscopic corrections from ETFSI [45] to those calculated using corrections from FRDM [44].

FIG. 5. Ratio of theoretical to experimental [50] neutron capture cross sections at 30 keV. Cross sections for light nuclei ($A < 30$) are not plotted because the statistical model cannot be applied in that region for neutron-capture reactions (compare Fig. 7).

FIG. 6. Deviation of the integration over the level density from the exact sum over levels, depending on the number of levels in the energy window. The full line describes a "worst case" with narrow resonances, the dotted line applies for broader resonances (e.g neutron s-waves).

FIG. 7. (Color) Stellar temperatures (in 10^9 K) for which the statistical model can be used. Plotted is the compound nucleus of the neutron-induced reaction n+Target. Stable nuclei are marked.

FIG. 8. (Color) Stellar temperatures (in 10^9) for which the statistical model can be used. Plotted is the compound nucleus of the alpha-induced reaction alpha+Target. Stable nuclei are marked.

FIG. 9. Stellar temperatures (in 10^9) for which the statistical model can be used. Plotted is the compound nucleus of the proton-induced reaction p+Target. Stable nuclei are marked.

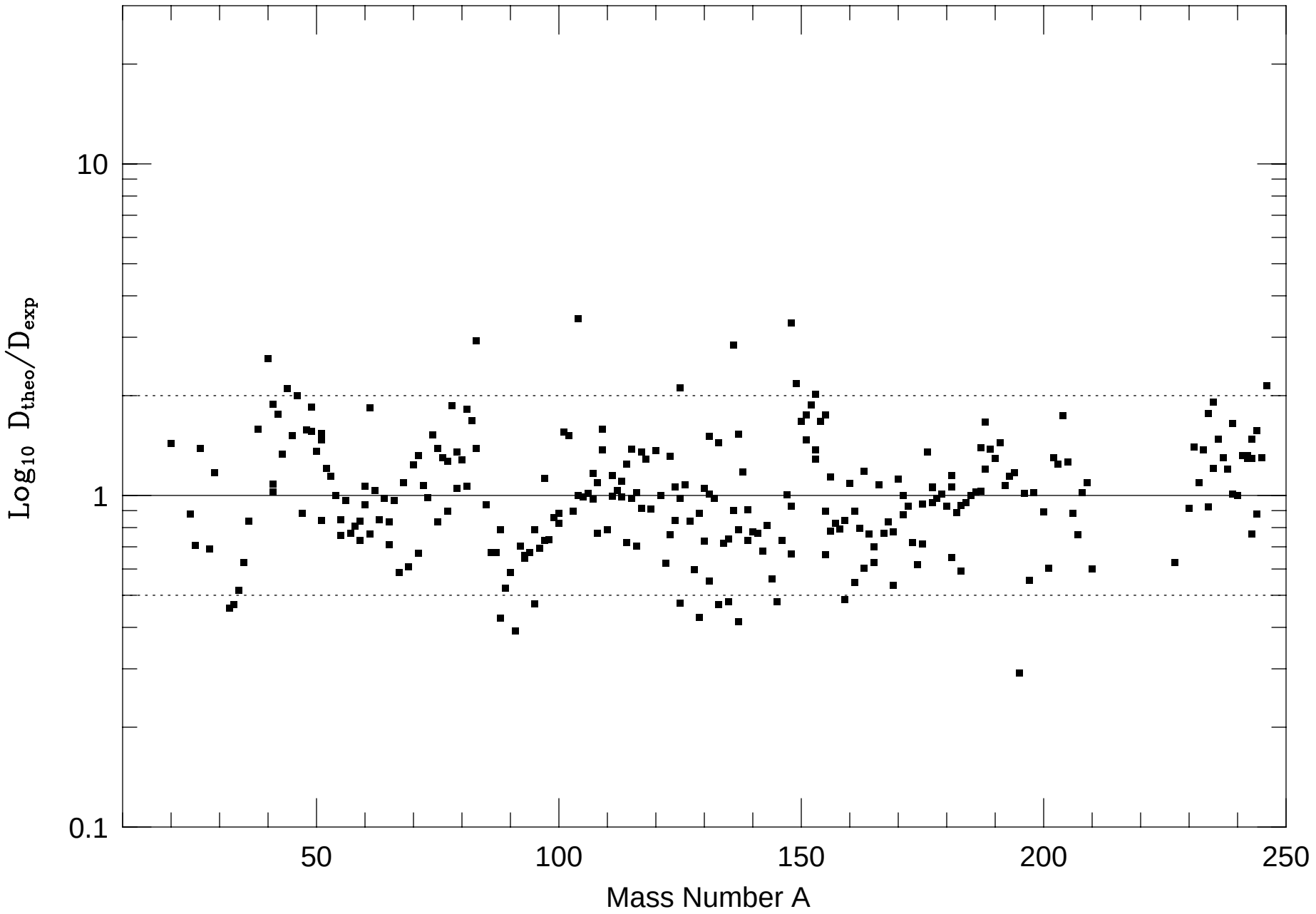
10
1
0.1
$\mathrm{Log}_{10}\ \mathrm{D}_{\mathrm{theo}}/\mathrm{D}_{\mathrm{exp}}$
50
100
150
200
250
Mass Number A

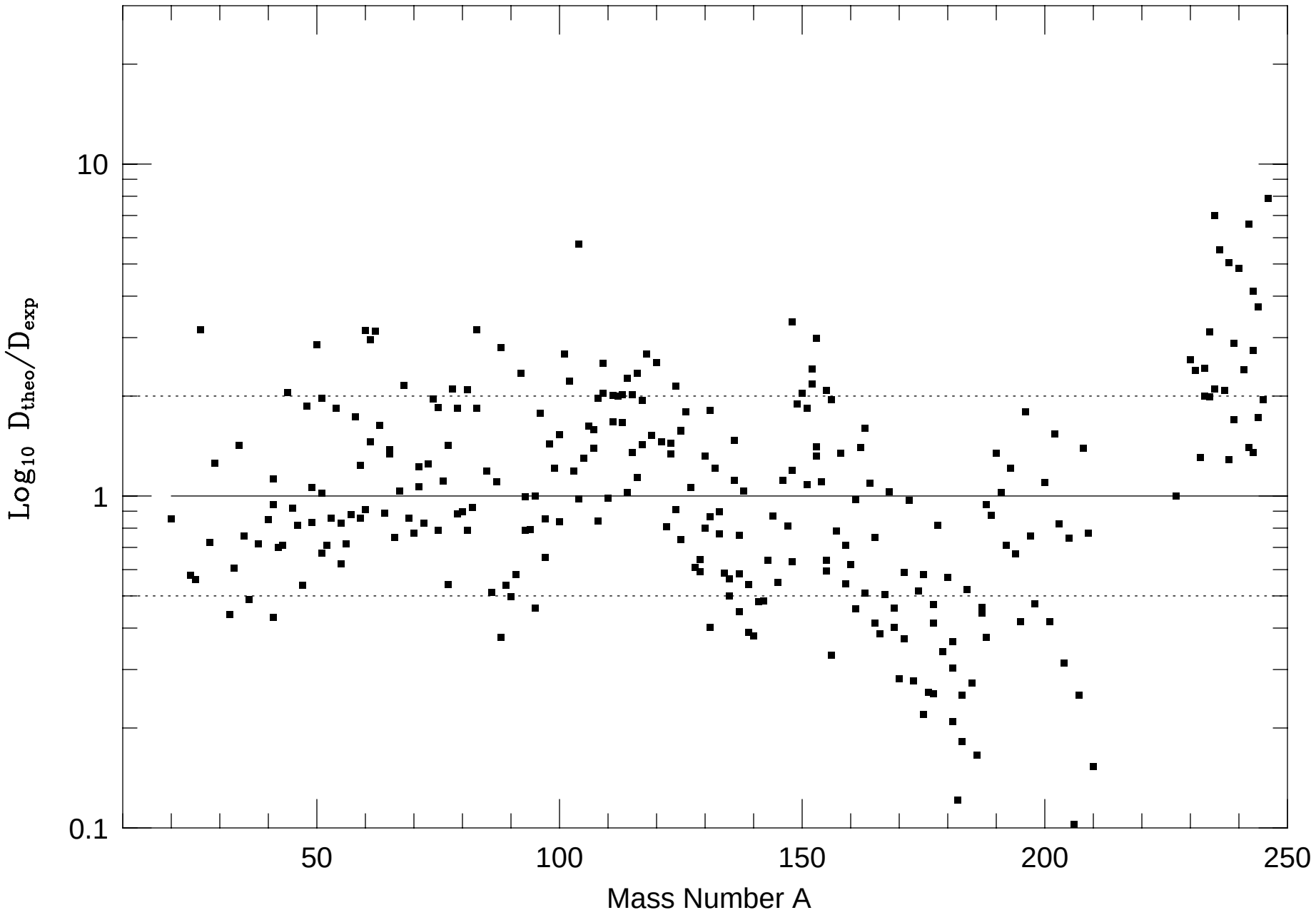
10
1
0.1
50
100
150
200
250
Mass Number A
Log10 Dtheo/Dexp

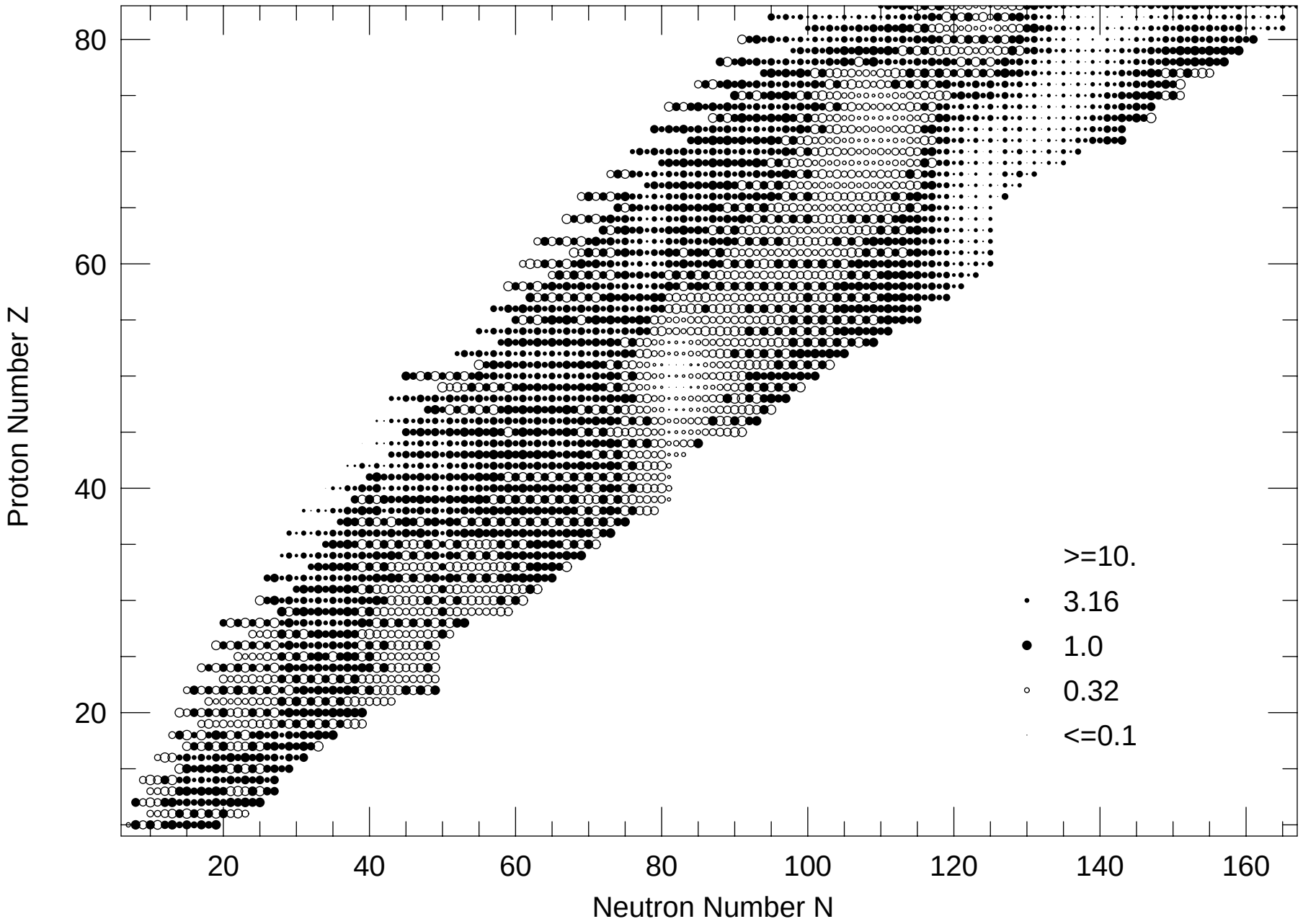
Proton Number Z
Neutron Number N
20
40
60
80
100
120
140
160
>=10.
3.16
1.0
0.32
<=0.1

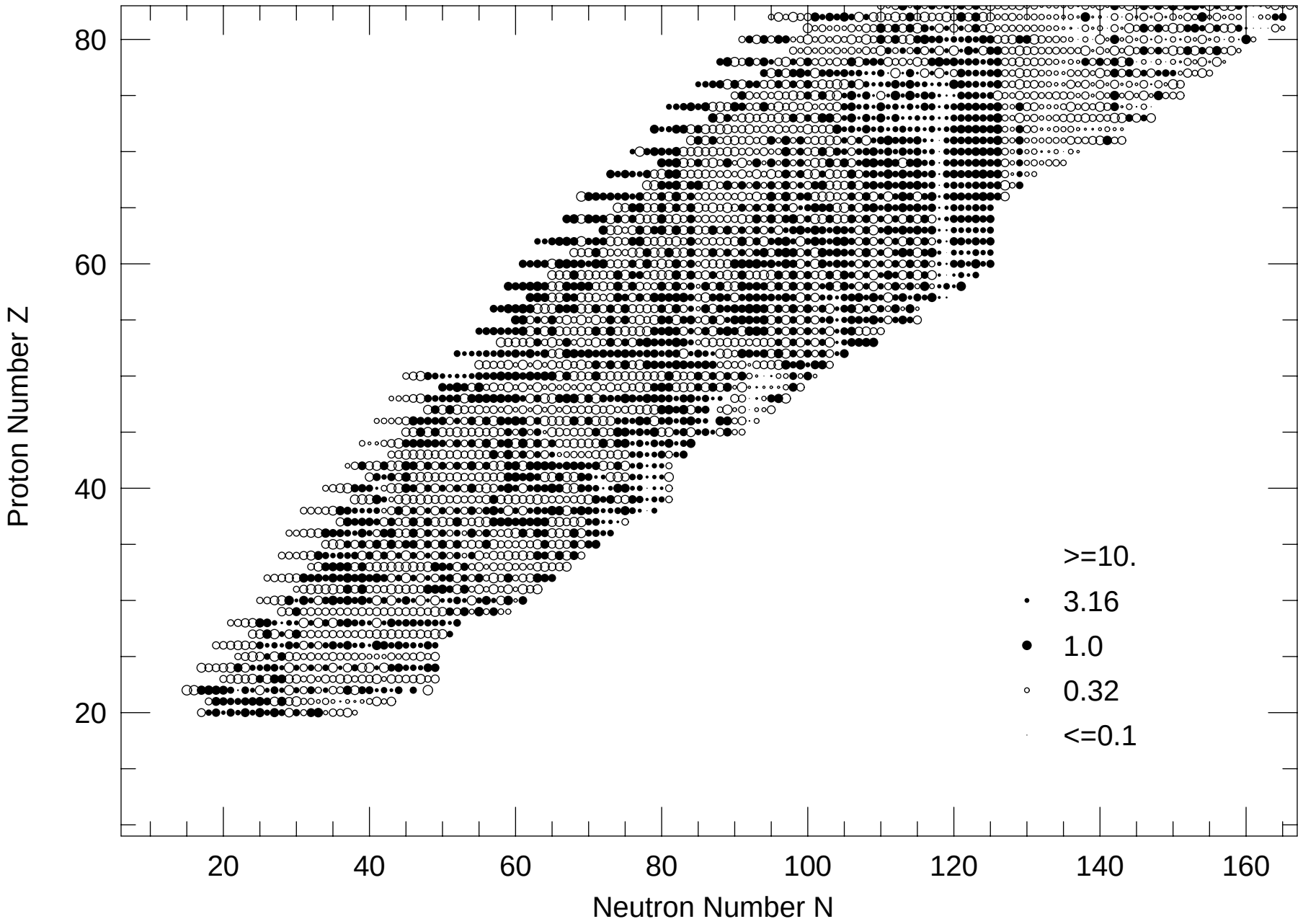
Proton Number Z
Neutron Number N
20
40
60
80
100
120
140
160
>=10.
3.16
1.0
0.32
<=0.1

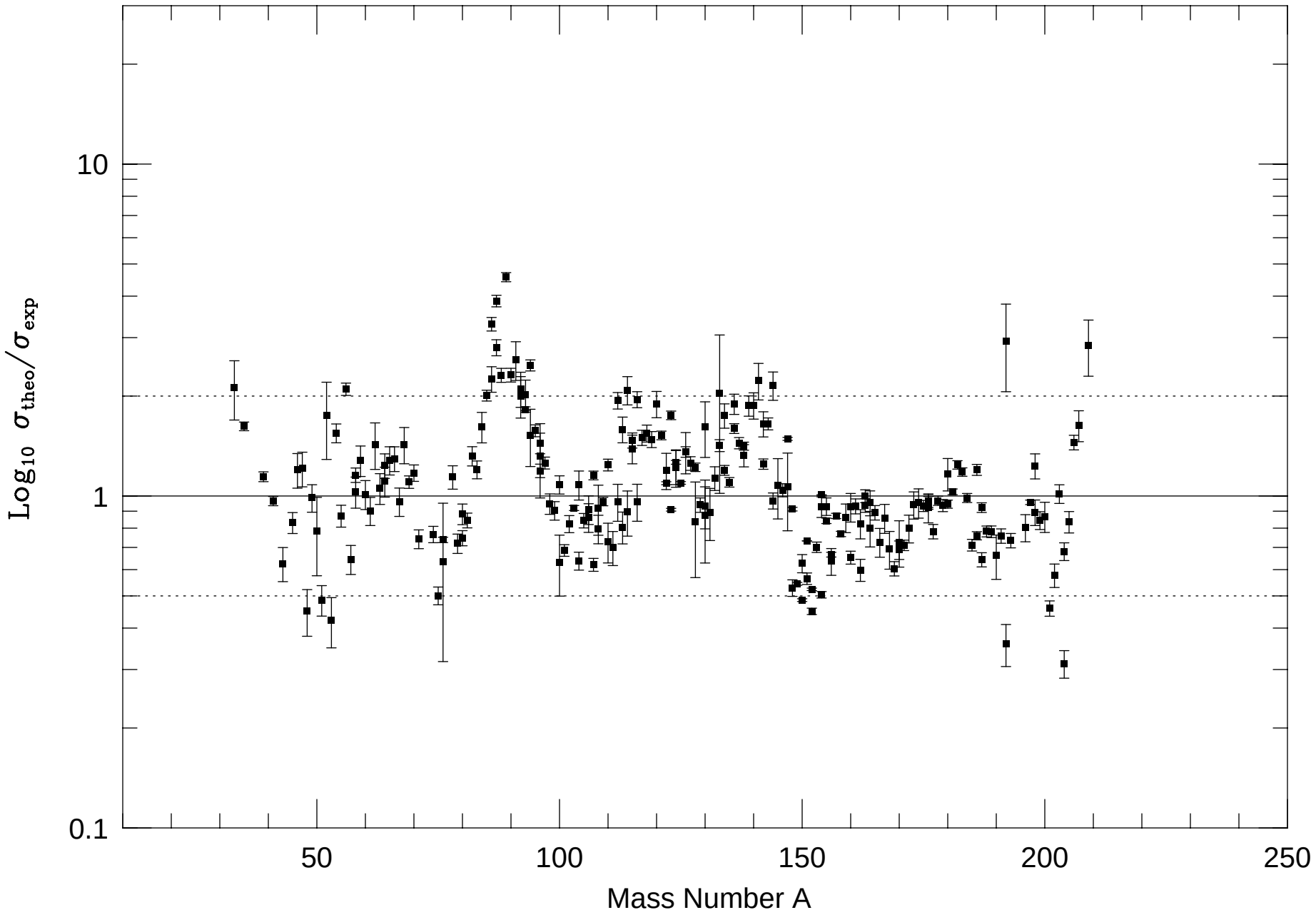
10
1
0.1
50
100
150
200
250
Mass Number A
Log10 σtheo/σexp

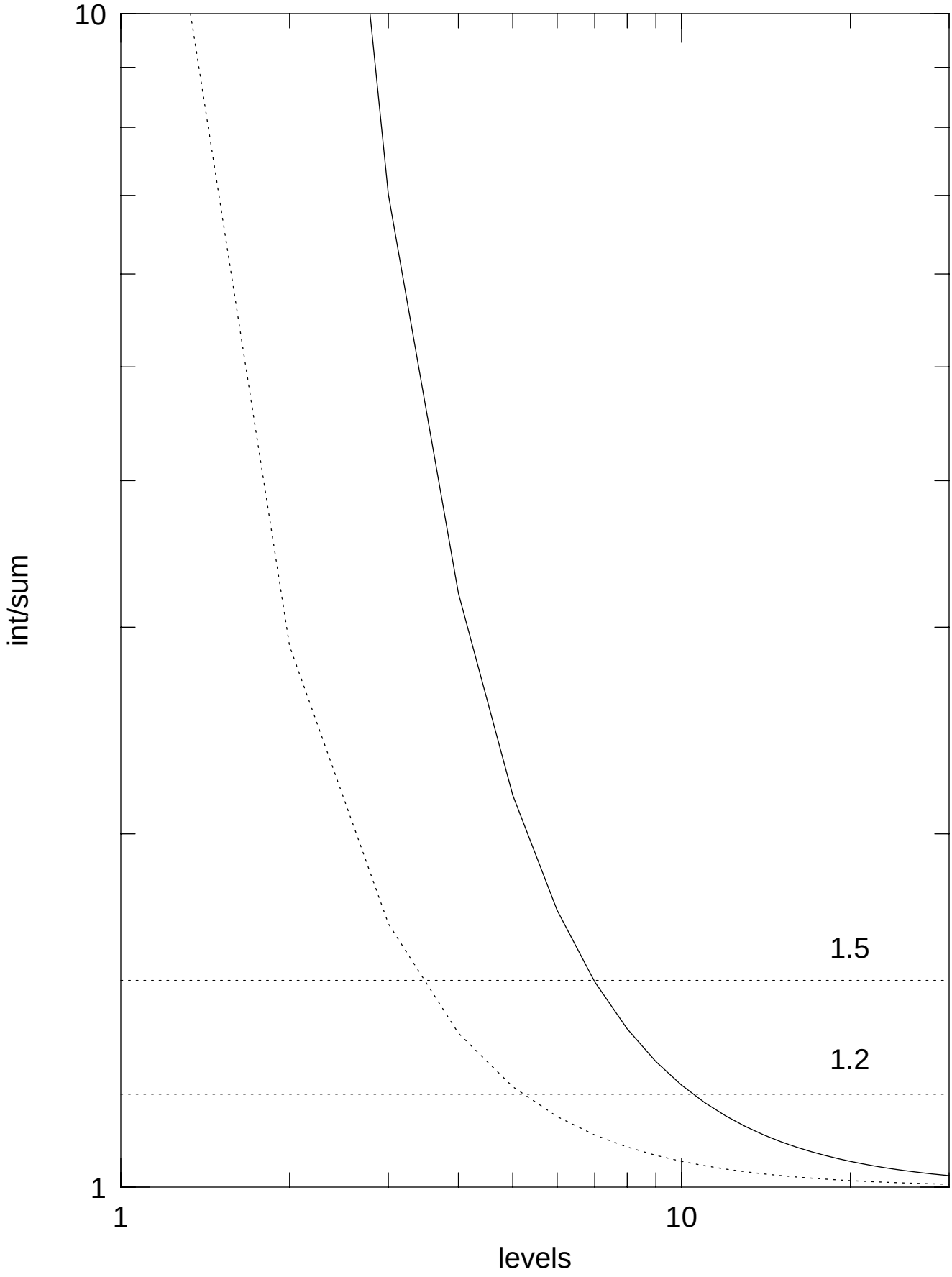
10
1
1
10
int/sum
levels
1.5
1.2

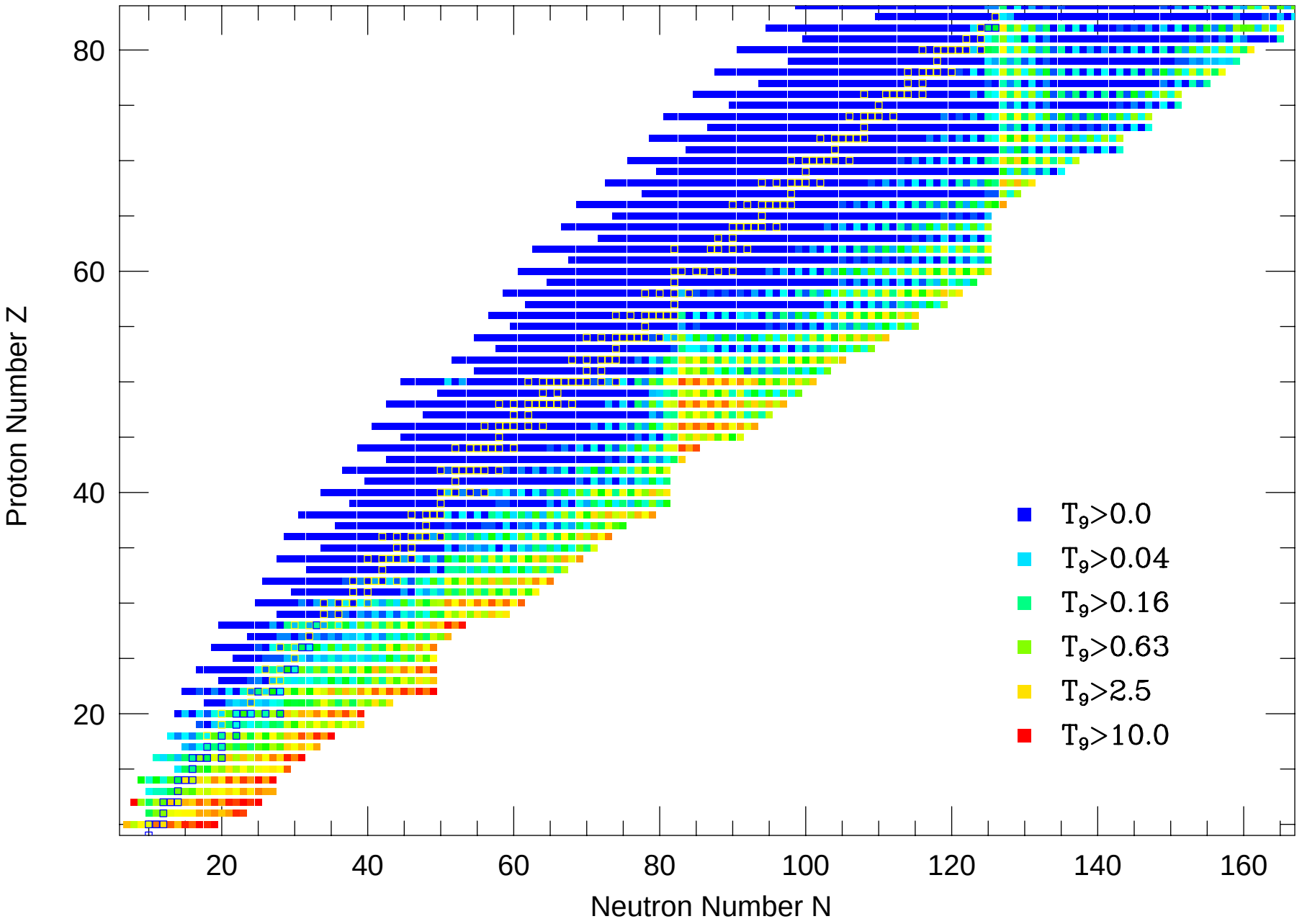
Proton Number Z
Neutron Number N
20
40
60
80
100
120
140
160
T_9>0.0
T_9>0.04
T_9>0.16
T_9>0.63
T_9>2.5
T_9>10.0

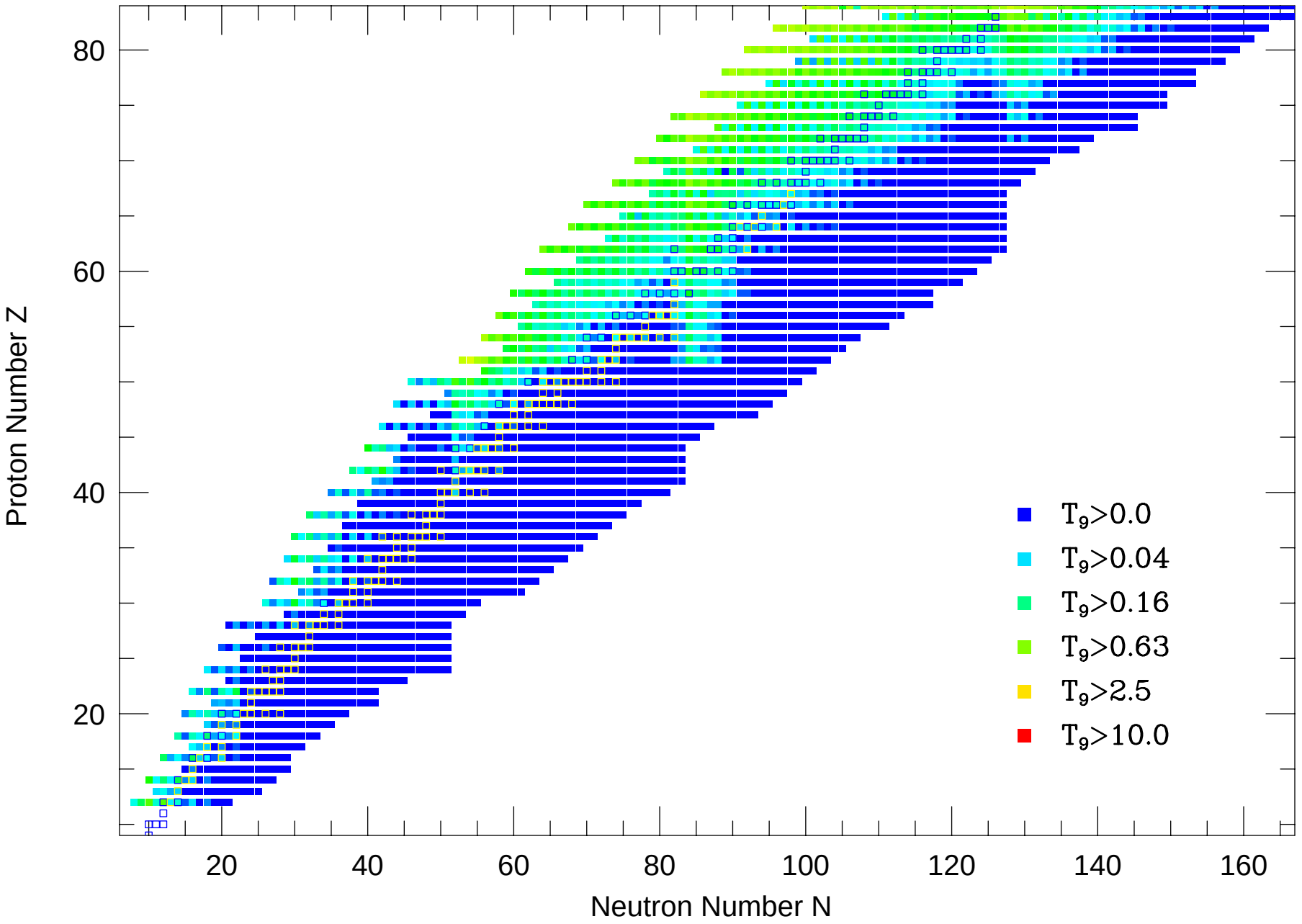
Proton Number Z
Neutron Number N
20
40
60
80
100
120
140
160
20
40
60
80
T_9>0.0
T_9>0.04
T_9>0.16
T_9>0.63
T_9>2.5
T_9>10.0

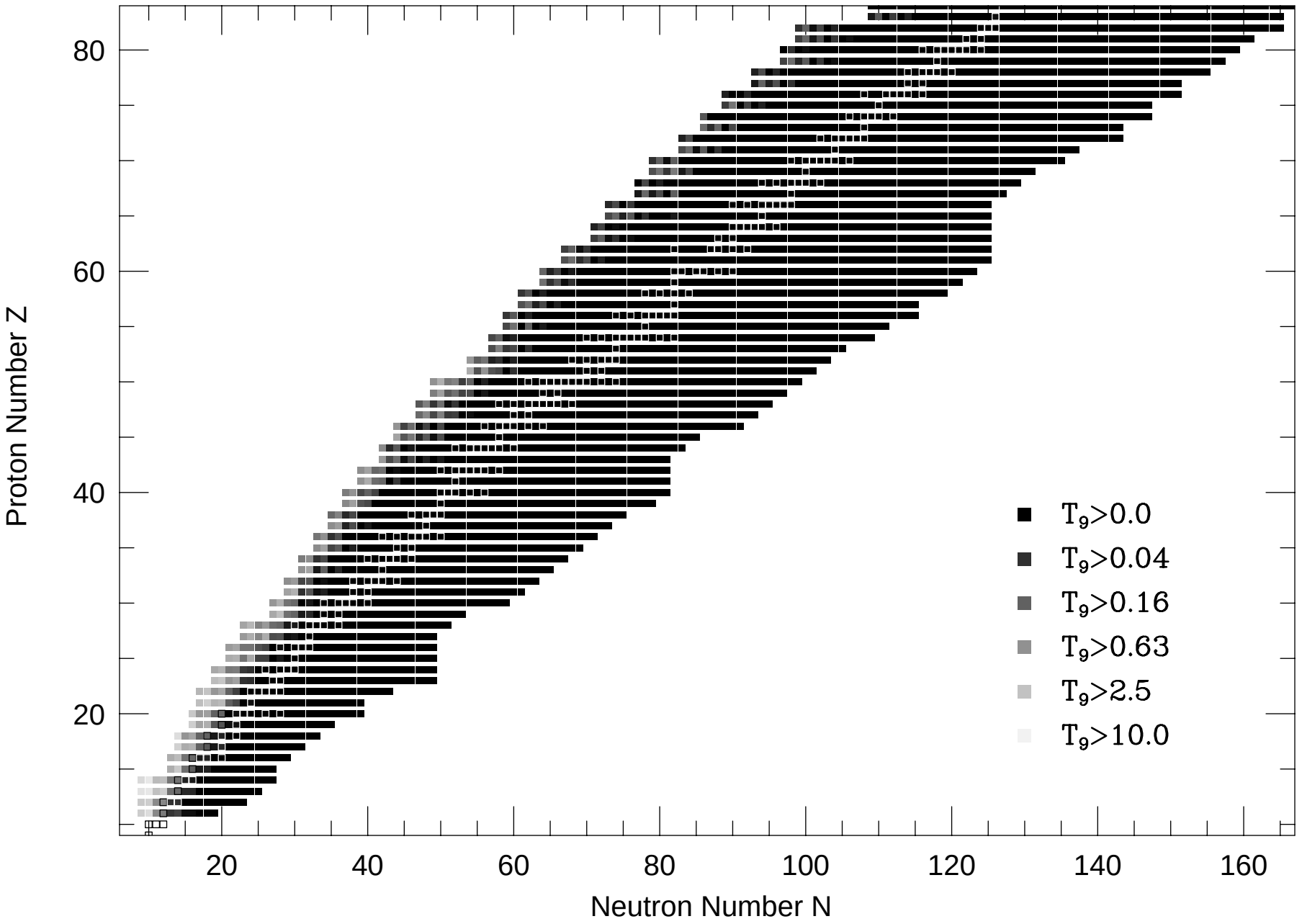
Proton Number Z
Neutron Number N
20
40
60
80
100
120
140
160
20
40
60
80
T_9>0.0
T_9>0.04
T_9>0.16
T_9>0.63
T_9>2.5
T_9>10.0